

## Change in stoichiometry of ZnS nanoparticles from the energy of action to nano- and femtosecond laser radiation

© A.S. Chernikov, D.A. Kochuev, A.A. Voznesenskaya, D.V. Abramov, K.S. Khorkov

Institute of Applied Mathematics Physics and Computer Science, Vladimir State University,  
600000 Vladimir, Russia

E-mail: khorkov@vlsu.ru

Received May 19, 2023

Revised July 11, 2023

Accepted October 30, 2023

In this paper, experiments on laser ablation of ZnS in atmospheric air using laser pulses with different energies and durations have been carried out. In the process of ablation processing, zinc sulfide nanoparticles with different stoichiometric ratio of elements were obtained. By varying the parameters, it is possible to control changes in the size of nanoparticles and their composition. As a result of studies of synthesized nanoparticles, Raman scattering spectra, energy dispersion analysis results, and images of deposited nanoparticles were obtained. Conclusions are drawn about the suitability of nanopowder synthesis approaches for the subsequent production of stable colloidal solutions.

**Keywords:** laser ablation, nanoparticles, colloidal solution, stoichiometry, zinc sulfide.

DOI: 10.61011/SC.2023.07.57417.5178C

At present, active research is being carried out in the direction of synthesis and application of spherical metal chalcogenide nanoparticles in biomedical applications [1]. Nanoparticles of this group can be successfully used in biomedicine. They are used in bioimaging, bio-probing, drug delivery, photothermal therapy [2,3]. In the listed directions, nanoparticles are used in the form of colloidal solutions. Colloidal solutions can be produced either by laser ablation in liquids or by adding nanoparticles to various dispersion media. Femtosecond laser ablation in liquid (FLAL) has attracted considerable attention because it has shown great potential in the synthesis of nanostructures such as quantum dots, nanoparticles [4,5], nanowires [6,7], nanoplates [8], etc. In process of synthesis of colloidal nanoparticles the phenomena of fragmentation of nanoparticles, coagulation of ablation products, change of chemical and phase composition of obtained nanomaterials are observed.

The method of synthesizing a colloidal solution of zinc sulfide (ZnS) is discussed in this work. This material is one of the widely used semiconductors and shows good properties for various applications [9]. The large band gap width of ZnS (2.6–4.6 eV) made it suitable for devices operating in the visible and ultraviolet ranges, such as sensors and bio-devices [10–14].

Bulk samples of polycrystalline ZnS were used in laser ablation experiments. The femtosecond laser complex TETA-10 (pulse duration 280 fs, pulse energy up to 150  $\mu$ J, pulse repetition rate 10 kHz, wavelength 1030 nm) and nanosecond laser (pulse duration 100 ns, pulse energy up to 1 mJ, pulse repetition rate 10 kHz, wavelength 1064 nm). The experimental scheme of obtaining ZnS nanoparticles by laser ablation is shown in Figure 1. Scanning by a laser beam generated by a laser source (1) over the surface of the ZnS (2) material to be treated, located on a sample holder

with an electrically insulating base (3), was performed by a galvanoscanner (4) equipped with a flat-field lens with a focal length of 200 mm. The scanning speed of the laser beam was 100 mm/s. The radiation was focused on the target surface into a spot with a diameter of 50  $\mu$ m. The laser ablation process took place in the working vessel (5). An electrostatic field was created in it by applying a high voltage (6–60 kV) from a source (7) to the electrodes (6) through high-voltage electrical inlets (8) located on the wall of the working vessel. The laser ablation process in the electrostatic field was recorded by a CCD camera (9) through a viewing window (10). As a result of laser action, the formation of ablated particles (11) was observed. Under the action of an electrostatic field, ablated particles were deposited on the surface of the substrates, behind which

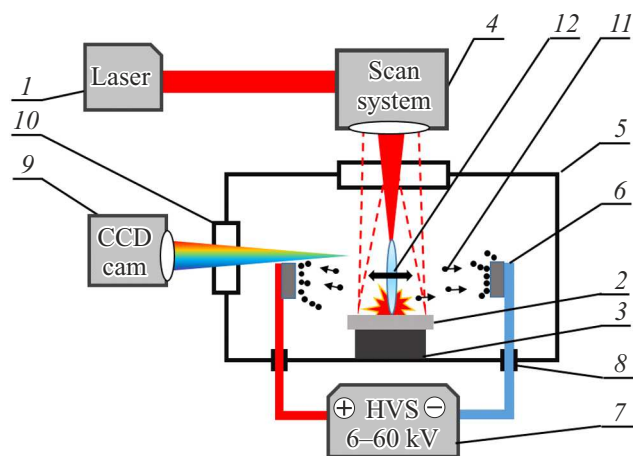


**Figure 1.** Experimental scheme for the preparation of ZnS nanoparticles by laser ablation. (The colored version of the figure is available on-line).

Parameters of the experiment on obtaining ZnS nanoparticles

Sample	Duration of pulse	Medium power, W	Density power, W/cm <sup>2</sup>	Stability solution	Component content, %		
					ZnS	ZnO	S
A	280 fs	1	$3.6 \cdot 10^{13}$	No	14.01	81.35	4.6
B	280 fs	0.3	$1.1 \cdot 10^{13}$	Yes	72.23	16.53	10.21
C	100 fs	20	$2.0 \cdot 10^9$	No	30.53	68	1.4

electrodes were placed. ZnS nanoparticles were deposited on the electrode surface as weakly agglomerated filaments consisting of spherical nanoparticles with dimensions of 5–150 nm. The glow intensity from the laser-induced plasma torch (12) increased when the high voltage source was turned off, which indicates that the ablated particles re-entered the band of laser beam propagation.

Zinc sulfide nanoparticles were produced by laser ablative fusion in atmospheric air under femtosecond laser irradiation (samples A and B) and nanosecond laser irradiation (sample C). The table shows the experimental parameters and the weight ratio of substances in the resulting samples. Colloidal solutions were prepared by transferring ZnS nanoparticles obtained from laser synthesis into deionized water. Next, the test tubes with the solution were subjected to ultrasonic treatment. The stability of the solution was checked by detecting precipitate at the bottom of the test tube. The presence of zinc oxide promotes the formation of zinc hydroxide upon interaction with water, which in turn promotes the coagulation of nanoparticles into a flake-like mass.

The scanning-electron microscope (SEM) images of the synthesized nanoparticles are shown in Figure 2. The investigated surface is a set of weakly agglomerated nanoparticles of spherical shape. A bimodal distribution is pronounced among the obtained nanoparticles. The synthesized particles have a size spread of 5–40 and 100–500 nm. The presence of large particles is caused by thermal and acoustic processes that contribute to the destruction of the polycrystalline material surface as a result of the cyclic stresses of laser pulse succession [15]. Large hot fragments become spherical in the dispersal process. The passage of ablated particles through the melting stage is confirmed by the change of wurtzite phase to sphalerite phase [16].

Figure 3 shows the Raman scattering (RS) of the obtained samples. The peak at  $219 \text{ cm}^{-1}$  corresponds to the longitudinal acoustic phonon of the 2nd order (2LA) ZnS. The broad response centered at  $280 \text{ cm}^{-1}$  consists of the unshared phonon modes  $A_1(\text{TO})$  and  $E_1(\text{TO})$  at  $272 \text{ cm}^{-1}$  and the phonon mode  $E_2(\text{TO})$  at  $284 \text{ cm}^{-1}$ . The peaks at  $336$  and  $350 \text{ cm}^{-1}$  correspond to the surface optical mode (SO) and the unshared phonon modes  $A_1(\text{LO})$  and  $E_1(\text{LO})$ . The spectra also show bands at  $380\text{--}450 \text{ cm}^{-1}$  associated with 2nd order spectra, as well as a weak response at  $600\text{--}700 \text{ cm}^{-1}$ . The presence of a peak at  $1000 \text{ cm}^{-1}$  and a weak band  $\sim 500 \text{ cm}^{-1}$  can be explained by the appearance

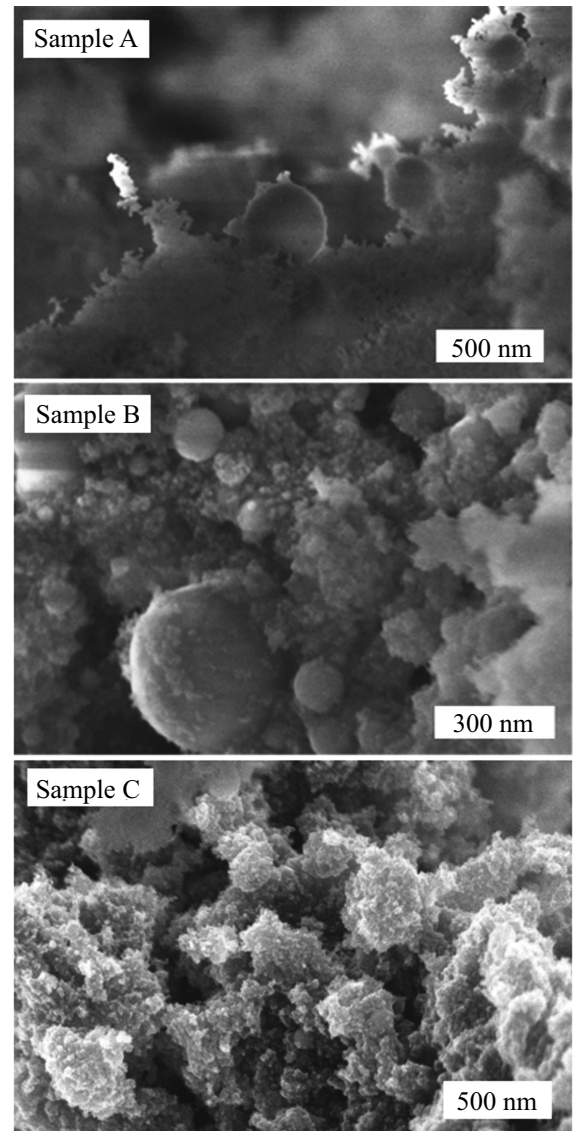


**Figure 2.** SEM images of ZnS nanoparticles obtained under different conditions.

of some zinc sulfate and zinc sulfate hydrate [17] on the surface of the ablation products due to the oxidation of ZnS by interaction with water vapor contained in the air.

The results of energy dispersive analysis of ZnS nanoparticles show the presence of oxygen (samples A and B) and indicate a change in the phase and chemical composition

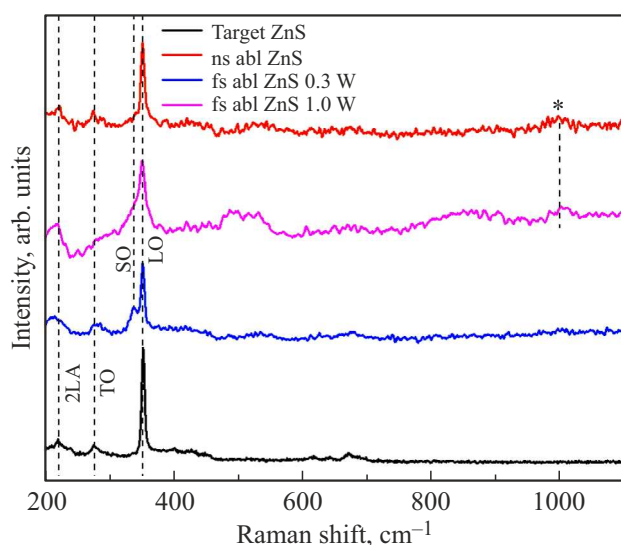


**Figure 3.** RSS spectra of ZnS nanoparticles.

of the original material (see table). Oxygen registration is related to the oxidation of zinc by air oxygen during ablative processes. Oxidative processes can be observed as a result of zinc sulfide dissociation during laser exposure, as well as due to the temperature effects of the laser-induced plasma channel. In the case of sample A, an intense laser-erosion plume and an extended laser-induced plasma channel were observed upon exposure to laser irradiation. In the case of sample B, the laser energy did not exceed the air breakdown threshold. In processing, the laser erosion plume was less pronounced, and the laser-induced plasma channel was recorded strictly above the surface of the ablated target. The presence of oxygen (sample B) may be due to the oxidation of the heated nanoparticle surface upon interaction with air oxygen.

The presence of oxygen is also evident in sample C. Here, the formation of zinc oxide during ablation of the starting material is observed as a result of thermal processes characteristic of material processing with nanosecond laser pulses. The lower zinc oxide content relative to sample A is due to the lower laser intensity. Probably, thermal oxidation processes of ablation products prevail under these conditions. The chain of processes of laser ablation and temperature evaporation of zinc sulfide is probably accompanied by dissociation of this compound and formation of zinc oxide and free sulfur. The formation of a zinc oxide shell on the surface of zinc sulfide nanoparticles in the case of samples A and C, which are similar in their properties despite the differences in synthesis modes, is not excluded. Obtaining stable colloidal systems is achieved by using zinc sulfide nano-powders with minimal zinc oxide content. Reducing the heating of the treated material and using inert gases can reduce the oxidation of nanoparticles ZnS.

## Funding

The study of the processes of formation of nanoparticles was supported by the Russian Science Foundation (grant No. 22-79-10348). The preparation and analysis of samples was carried out within the framework of the State Assignment of the Ministry of Science and Higher Education of the Russian Federation, topic FZUN-2020-0013.

## Conflict of interest

The authors declare that they have no conflict of interest.

## References

- [1] A.S. Chernikov, G.I. Tselikov, M.Yu. Gubin, A.V. Shesterikov, K.S. Khorkov, A.V. Syuy, G.A. Ermolaev, I.S. Kazantsev, R.I. Romanov, A.M. Markeev, A.A. Popov, G.V. Tikhonovsk, O.O. Kapitanova, D.A. Kochuev, A.Yu. Leksin, D.I. Tselikov, A.V. Arsenin, A.V. Kabashin, V.S. Volkov, A.V. Prokhorov. *J. Mater. Chem.*, **11** (10), 3493 (2023).
- [2] M. Ensoylu, H. Atmaca, A.M. Deliormanli. *J. Aust. Ceram. Soc.*, **58** (2), 397 (2022).
- [3] K. Manzoor, S. Johny, D. Thomas, S. Setua, D. Menon, S. Nair. *Nanotechnol.*, **20** (6), 065102 (2009).
- [4] L. Liao, Q. Zhang, Z. Su, Z. Zhao, Y. Wang, Y. Li, X. Lu, D. Wei, G. Feng, Q. Yu, X. Cai, J. Zhao, Z. Ren, H. Fang, F. Robles-Hernandez, S. Baldelli, J. Bao. *Nature Nanotechnol.*, **9**, 69 (2014).
- [5] Z. Ye, L. Kong, F. Chen, Z. Chen, Y. Lin, C. Liu. *Optik*, **164**, 345 (2018).
- [6] G. Feng, C. Yang, S. Zhou. *Nano Lett.*, **13** (1), 272 (2013).
- [7] C. Yang, J. Yin, J. Dai, S. Wang, H. Zhang, G. Feng, S. Zhou. *Chem. Lett.*, **45** (7), 755 (2016).
- [8] H. Zhang, G. Duan, Yu. Li, X. Xu, Z. Dai, W. Cai. *Cryst. Growth Des.*, **12** (5), 2646 (2012).
- [9] X. Fang, T. Zhai, U.K. Gautam, L. Li, L. Wu, Y. Bando, D. Golberg. *Progr. Mater. Sci.*, **56** (2), 175 (2011).
- [10] H. Azimi, M. Ghoranneviss, S. Elahi, R. Yousefi. *Ceram. Int.*, **42** (12), 14094 (2016).
- [11] T.W. Sung, Y.L. Lo. *Sensors Actuators B: Chem.*, **165** (1), 119 (2012).
- [12] Y.C. Chen, C.H. Wang, H.Y. Lin, B.H. Li, W.T. Chen, C.P. Liu. *Nanotechnol.*, **21** (45), 455604 (2010).
- [13] U.E. Kurilova, A.S. Chernikov, D.A. Kochuev, L.S. Volkova, A.A. Voznesenskaya, R.V. Chkalov, D.V. Abramov, A.V. Kazak, I.A. Suetina, M.V. Mezentseva, L.I. Russu, A.Yu. Gerasimenko, K.S. Khorkov. *J. Biomed. Photon. Eng.*, **9** (2), 020301 (2023).
- [14] N. Kaur, S. Kaur, J. Singh, M. Rawat. *J. Bioelectron. Nanotechnol.*, **1** (1), 5 (2016).
- [15] A.A. Ionin, S.I. Kudryashov, L.V. Seleznev, D.V. Sinitsyn, A.F. Bunkin, V.N. Lednev, S.M. Pershin. *J. Exp. Theor. Phys.*, **116**, 347 (2013).
- [16] A.S. Chernikov, D.A. Kochuev, A.A. Voznesenskaya, A.V. Egorova, K.S. Khorkov. *J. Phys.: Conf. Ser.*, **2077** (1), 012002 (2021).
- [17] W.W. Rudolph, M.H. Brooker, P.R. Tremaine. *J. Solution Chem.*, **28** (5), 621 (1999).

*Translated by Ego Translating*